CHINESE OPTICS LETTERS

Vol. 22, No. 2 | February 2024

All-optical suppression on the impact of Sun outage in laser satellite communication systems by using a nonlinear semiconductor optical amplifier

Xiaoliang Li (李晓亮)[1,2**], Rongke Liu (刘荣科)[1*], and Feng Fan (范 峰)[2]

[1] School of Electronics and Information Engineering, Beihang University, Beijing 100191, China

[2] Beijing Research Institute of Telemetry, Beijing 100094, China

*Corresponding author: rongke_liu@buaa.edu.cn

**Corresponding author: lix79@163.com

Received September 10, 2023 | Accepted September 22, 2023 | Posted Online February 20, 2024

We introduce an all-optical approach, optical parametric amplification (OPA) processor to suppress the impact of Sun outage in laser satellite communication systems, which is implemented by only one nonlinear semiconductor optical amplifier driven by both electrical and optical pumps. The optimized OPA processor, with a current of 539 mA and a pump-to-signal ratio of 16 dB, could significantly improve the signal quality by 3.5 dB in experiments for the elevation angle of Sun radiation of 0 rad. The signal quality improvement is observed in the whole range of the elevation angle, confirming the effectiveness of the proposed OPA processor in the field of Sun radiation mitigation.

Keywords: nonlinear optics; Sun outage; laser satellite communication.

DOI: 10.3788/COL202422.020602

1. Introduction

With the rapid implementation of low-Earth orbit (LEO) satellites, the giant LEO constellation is a promising candidate for next-generation backbone networks, delivering the capability of high capacity and performing multiple tasks across the whole Earth[1]. Meanwhile, the transmission technology with the laser as the carrier has potential advantages, such as wideband operation, over a hundred gigabits data speed capability, and the information safety that has been applied in current satellites[2,3]. In recent investigations, over 200 Gbit/s of space-to-ground communication has been achieved[4], and laser terminals for intersatellite transmissions[5] have performed successfully, suggesting the high-capacity transmission capability of these laser systems. However, the high signal-to-noise ratio (SNR) of optical signals is critical to such high-speed communication, especially when the advanced modulation format is applied[6]. In free-space laser transmission systems, multiple distortion sources, such as the Doppler frequency shift, platform vibration, and Sun outage, could severely degrade signal quality. To improve the transmission performance, the digital signal processing (DSP) approach has been adopted into satellite receiving subsystems to mitigate the impact from frequency shifts and power vibrations[7,8]. But the Sun outage as random noise, which could interrupt or even block laser communication by radiation, unfortunately could not be compensated through DSP algorithms. Therefore, the significant reduction of the impact from the Sun outage is still an open issue for laser satellite communication systems (LSCSs).

To mitigate the impact of Sun outage, several methods have been proposed, e.g., the use of the Sun shelter[9] or selecting an alternative path. The Sun shelter method could block the radiation from the off-axis direction, reducing the unwanted light input into the laser antenna. Consequently, the received optical SNR (OSNR) is indeed increased through the shelter. But this method could not reduce the light along the propagating direction of the laser path, not even the in-band random noise falling into the communication window, which is the major distortion affecting LSCSs. Selecting an alternative route is also an effective way to avoid interrupting communication due to Sun outage. However, such a method increases the routing pressure, which becomes worse when complex networking is applied over LEO mega-constellations. Therefore, reducing the impact of Sun outage, especially the distortion from the in-band radiation noise, is an essential function in laser-based satellites. Considering the nature of laser communication, a novel approach with less complexity should also be operated in the optical domain.

All-optical signal processing (AOSP) technology is a promising solution to suppress the signal distortion directly in the optical domain[10]. The nonlinear devices that are used in AOSP are essential to their implementation. There are two groups of

these nonlinear devices: passive elements and active elements. The passive devices, e.g., highly nonlinear fibers (HNLFs), periodically poled lithium niobate (PPLN), and silicon waveguides, require several watts or hundreds of microwatts at optical levels to stimulate the designed nonlinearity[11–13]. Therefore, in view of their power consumption, an active device is more practicable in satellite implementation. The nonlinear semiconductor optical amplifier (SOA) is a powerful element to perform multiple optical nonlinearities, including optical parametric amplification (OPA), four-wave mixing (FWM), and cross-gain modulation (XGM)[14–16]. In this Letter, we used only one nonlinear SOA to suppress the impact of Sun outage on the quadrature-phase-shift-keying (QPSK)-based laser satellite communication. According to the experimental investigation, around 3.5 dB signal quality improvement was observed through the OPA process in the nonlinear SOA, confirming the suppressing capability of the proposed scheme on the in-band distortion from Sun outage.

2. Theoretical Model

The SOA is a compact solution to perform the AOSP through multiple nonlinear effects. According to the requirement of the wavelength consistency in LSCS, the OPA process is used to mitigate the impact of Sun outage, where the wavelength of signals before and after the all-optical processor stays the same. Through squeezing the signal distortion in the optical domain, the OPA has been implemented into the field of signal regenerations[17–19]. Most research works focus on the conventional on–off keying (OOK) format. In this Letter, we reveal the mitigation performance on Sun outage by putting an OPA processor into the satellite. After the OPA process, the input signal A_s could be evaluated in a nonlinear SOA as follows[20]:

$$\frac{\mathrm{d}A_s}{\mathrm{d}z} = \frac{1}{2}\{[\Gamma g_{\mathrm{ms}}(1 - i\alpha_m) - \alpha_0] - \Gamma g_{\mathrm{ms}}(\eta_{sp}|A_p|^2 + \eta_{sx}|A_x|^2)\}A_{\mathrm{in}} - \Gamma\frac{g_{\mathrm{ms}}}{2}(\eta_{px}A_p^2A_x^*e^{-i\Delta kz}), \quad (1)$$

where A_i ($i = s$, p, and x) represents the signal, pump, and idler, respectively; Γ is the confinement factor; g_{ms} is the material gain; α_m is the linewidth enhancement factor; α_0 is the loss coefficient; η_{ij} ($i, j = s, p, x$) is the nonlinear coupling coefficient; and the mismatching factor Δk could be zero for the SOA case. Based on Eq. (1), the parametric gain is dependent on both the optical pump A_p and the electrical pump (the current through g_{ms}). In the experiment, we investigated the impact of the two pumps (electrical and optical) on the OPA processor-based Sun outage mitigator.

3. Experimental Setup

The experimental setup for the OPA processor-based Sun-outage mitigator is depicted in Fig. 1(a). The system is composed of four parts: the QPSK generator, the Sun radiation emulator, the all-optical OPA processor, and the coherent receiver (Co-Rx). In the QPSK generator, a continuous-wave (CW) light with the length of $\lambda_{33} = 1550.92$ nm [Ch33 in dense wavelength-division-multiplexing (DWDM) grid] was launched into an I/Q modulator (IQM), which was driven by two 10 Gbit/s non-return-to-zero (NRZ) electrical data as I and Q parts generated by an arbitrary waveform generator (AWG). The state of polarization (SOP) of the input CW light was adjusted by polarization controller 1 (PC-1) to achieve the polarization matching. A 99:1 optical splitter 1 (OS-1) was placed at the output of the IQM to monitor the power level, enabling achieving the best modulation performance through tuning the three bias currents in the IQM. In the Sun radiation emulator, the noise was generated by a wideband optical source because similar spectral characteristics are obtained from Sun radiation and this amplified-spontaneous-emission (ASE) source in the C-band. The maximal output of the wideband optical source was about 0 dBm. The strength of the Sun radiation emulator was adjusted by a variable optical attenuator (VOA-1) to simulate the changes of the elevation angle from the Sun. Meanwhile, the optical power of QPSK signals was amplified by an erbium-doped fiber amplifier (EDFA) to maintain a proper OSNR in the test. A 3 dB optical coupler (OC-1) was used to couple the two lights to generate the distorted optical QPSK signal. An optical spectrum analyzer (OSA) was placed at the 1% output port of the 99:1 OS-2 to monitor the OSNR value of the distorted signals. In the all-optical OPA processor unit, a nonlinear SOA element

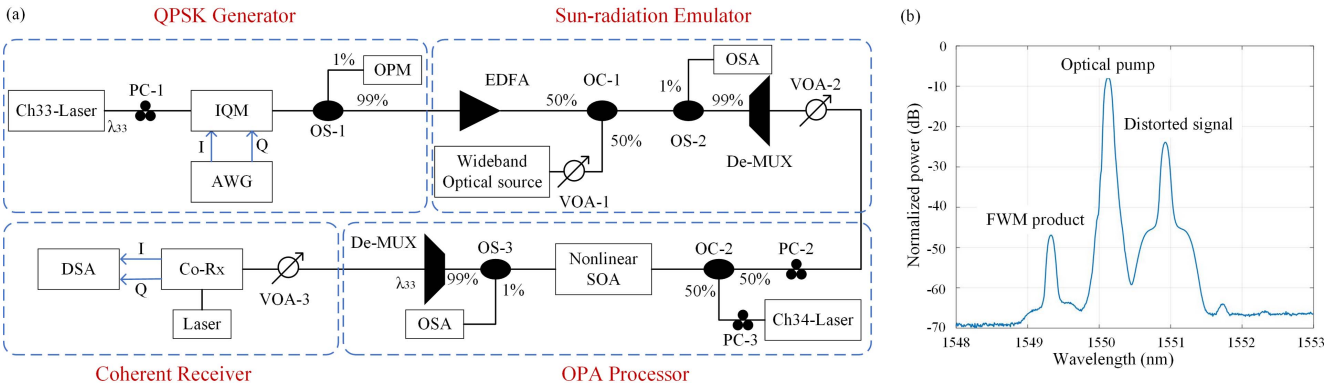

Fig. 1. (a) Experimental setup for the OPA processor-based Sun-outage mitigation; (b) optical spectrum obtained from the nonlinear SOA element.

was used to stimulate the OPA process. In such a process, another CW light as the optical pump was also input into the SOA. The wavelength of this optical pump was 1550.12 nm, Ch34 in the DWDM grid. At the output of SOA, a 99:1 OS-3 was used to extract 1% of the light to monitor the OPA process from the nonlinear OSA. By adjusting PC-2 and PC-3, the highest FWM product was obtained, suggesting the best OPA also happened. The optical spectrum obtained from the output of SOA is depicted in Fig. 1(b). A clear FWM product was observed in the experimental test, proving the OPA happened when the two inputs, i.e., the distorted QPSK and the optical pump, were simultaneously launched. A DWDM demultiplexer (De-MUX) that had the same wavelength as the input signal was used to extract the regenerated signal. In the coherent receiving unit, a VOA-3 was placed at the input port of the Co-Rx as a power limiter to avoid exceeding the receiving level after the optical amplifying process. The local laser with the same wavelength as the input signal was also launched into the Co-Rx. Simple DSP algorithms were used to perform the basic functions, (e.g., the frequency offset estimation and the phase compensation) to restore the QPSK signals. No equalization behaviors were included during the DSP processing.

4. Results and Discussion

First, we carry out the electrical pump optimization for the OPA processor. The SOA performance of optical amplification is dependent on the current of the electrical pump. In our experiment, the output power of the nonlinear SOA is also sensitive to the current. In Fig. 2(a), the measured data for the undertested SOA is depicted when the electrical pump is solely applied. The maximal output was over 10 dBm, and clear saturation was observed when the current was larger than 300 mA. Moreover, we also tested the dependence of the OPA performance on the current. In this case, both the electrical and optical pumps were applied onto the nonlinear SOA. The signal quality of the OPA product was measured, as depicted in Fig. 2(b). The input signal quality Q^2 of the QPSK signal was about 16.8 dB. To give a fair comparison, the optical power input into the Co-Rx was fixed for the whole test. According to the tested results, the signal quality was improved by almost 1 dB when the current was in the range of 200 to 539 mA. Therefore, the electrical pump for the OPA processer-based Sun-outage mitigator was set as 539 mA in the subsequent investigations. Based on the configuration of the experimental setup, we built a simulation platform through VPI to evaluate the performance of the proposed OPA processor. The parameters we used in the simulation were the same as in the experiment. The results (depicted with blue lines) are plotted in Fig. 2. The similar outputs obtained from both experiment and simulation further confirm the correctness of the model and the scheme of the nonlinear SOA.

Next, we discuss the impact of the optical pump on the OPA processor. When the current was fixed at 539 mA, we swept the input power from −19 to 5 dBm and collected the output power of the OPA product; see the results in Fig. 3(a). The optical pump

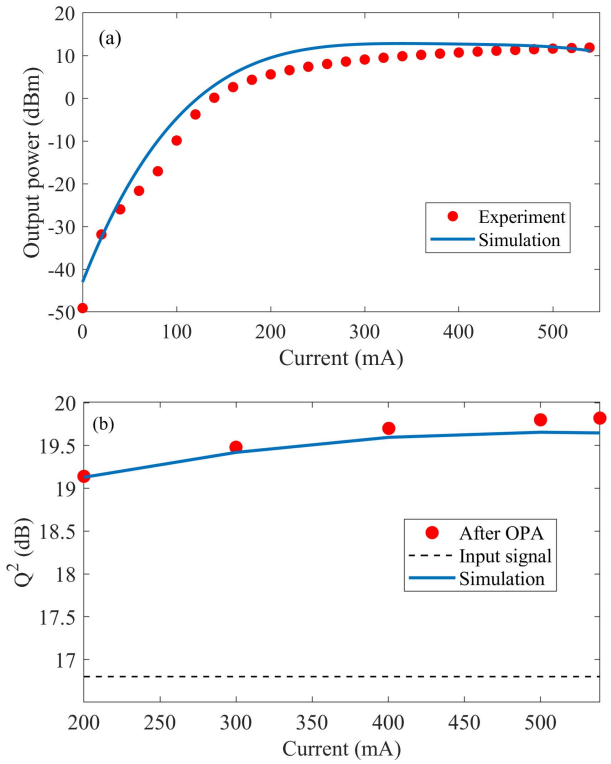

Fig. 2. (a) Dependence of the output power on the current; (b) current dependence of the OPA processor.

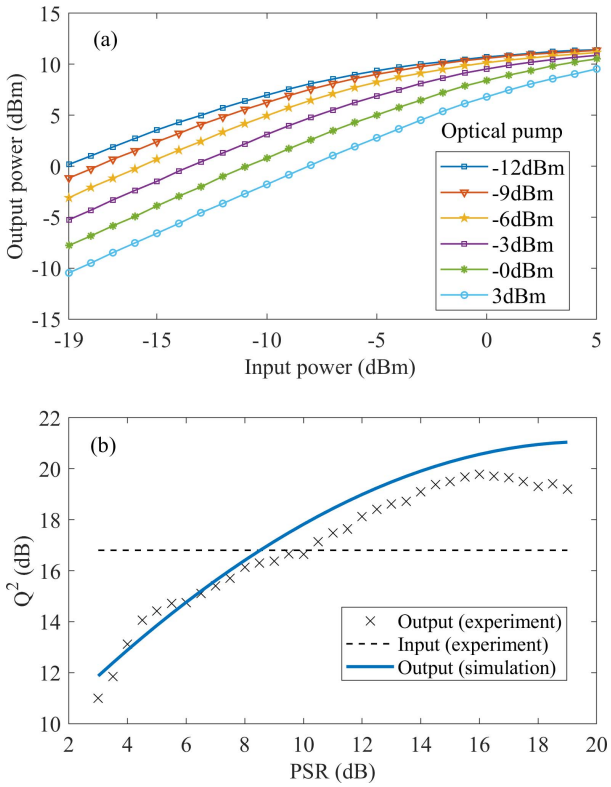

Fig. 3. (a) Power response between input and output signals from the OPA; (b) PSR dependence of the OPA processor.

was selected in the range of −12 to 3 dBm. The optical pump-CW light was fixed to each curve, the values given in the legend of the figure. The power saturation behavior was observed from the nonlinear input-to-output power response, suggesting the amplitude suppression obtained from the OPA. The plateau becomes much wider when the optical pump is low. However, the CW pump could not suppress the pattern effect of SOA. We need to select the proper power levels for both pump and signal. To achieve the balance between the suppression on the pattern effect and the amplitude mitigation from the nonlinear response, we optimized the pump-to-signal ratio (PSR) in this OPA processor. In the experiment, we kept the pump power as 3 dBm and swept the optical power of the distorted QPSK signals by tuning VOA-2. Figure 3(b) depicts the measured and simulated results when the input PSR is changed. When the CW pump was increased, the pattern effect was clearly suppressed due to the reduction of the input power variation. Moreover, the higher nonlinear gain through the OPA process was naturally expected when the optical pump was enhanced. Furthermore, the nonlinear response from input-to-output power facilitated the all-optical approach in suppressing the amplitude distortion, enabling increased signal quality directly in the optical domain. Consequently, better output was collected from the nonlinear SOA. According to the test results, the pattern effect could be well suppressed when the PSR was larger than 10.5 dB, in which the output quality was better than the input quality, and the best output was achieved at the input PSR of around 16 dB. Therefore, the input PSR was fixed at 16 dB in the OPA processor-based Sun-outage mitigator.

Finally, we investigated the mitigation performance of the optimized OPA processor for the impact on Sun outage. Because of the long distance between the Sun and Earth, the strength of the Sun's radiation could be considered as the fixed value. But the received noise at the antenna was indeed changed following the variation of the elevation angle. In the experiment, we tuned the output power from the Sun-radiation emulator and calculated the corresponding elevation angle according to the received radiation strength. Then we could simulate the scenario of the Sun outage happening in LSCSs. The results are depicted in Fig. 4. According to the experimental results, the most severe impact happened at the elevation angle $\theta_s = 0$ rad, resulting in the worst Q^2 of distorted signals, close to 14.1 dB. In this case, the OPA processor performed the best signal quality improvement, achieving a 3.5 dB enhancement. By increasing the value of the elevation angle, the distortions coming from Sun outage became weak; see the blue marks in Fig. 4. For the case of $\theta_s = \pi/2$ rad, the received noise was close to zero, suggesting no Sun outage happened in the laser system. Even in such a case, the OPA processor could improve the signal quality by about 1 dB, proving the suppression capability of the all-optical approach in LSCSs. Therefore, quality improvement was achieved in the whole tested elevation-angle range by suppressing the in-band radiation noise. The output results are depicted in Fig. 4 as the red marks. We also simulated the suppression behavior of the proposed OPA processor. The lines

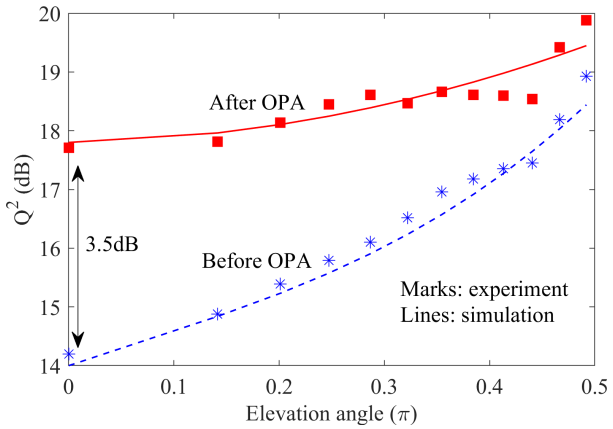

Fig. 4. Signal quality improvement before and after the OPA processor when the QPSK signals are distorted by Sun outage.

depicted in Fig. 4 share the same trend as the experiment, confirming the all-optical regeneration in the LSCS. It should be noted that less improvement should be expected if the strength of the Sun's radiation was further increased because the regeneration range of the proposed OPA processor would limit the performance.

5. Conclusion

We introduce an all-optical approach OPA processor into the satellite payload to suppress the impact of Sun outage, which could deal with the most severe distortion from in-band radiation noise. According to the experimental test, the best improvement of 3.5 dB was obtained at the elevation angle of 0 rad, which was also the worst case of Sun outage. When sweeping the whole range of elevation angle, more than 1 dB signal quality improvement was achieved by the OPA processor, confirming the suppression function through the proposed all-optical approach. To the best of our knowledge, this is the first experiment in which an OPA was used to suppress the impact of Sun outage. This all-optical nonlinear amplifier offers a potential combination in which both power restoration and signal processing could happen in only one device, providing a low power consumption solution to LSCS.

Acknowledgements

This work was supported by the National Key Research and Development Program of China (No. 2022YFB2803205) and the National Basic Research Project (No. JCKY2020560B001).

References

1. J. Zhang, Y. Cai, C. Xue, *et al.*, "LEO mega constellations: review of development, impact, surveillance, and governance," Space Sci. Technol. **2022**, 9865174 (2022).
2. S. Arnon and N. S. Kopeika, "Laser satellite communication network-vibration effect and possible solutions," Proc. IEEE **85**, 1646 (1997).

3. B. Robert, A. J. Miguel, and L. Alexander, "Progress in satellite quantum key distribution," NPJ Quantum Inf. **3**, 30 (2017).
4. C. Q. Choi, "NASA's laser link boasts record-breaking 200-Gb/s speed," https://spectrum.ieee.org/laser-communications (May 29, 2023).
5. Y. Qiao, T. Li, H. Li, *et al.*, "Design and verification of high-speed inter-satellite laser communication terminal," Opt. Commun. Technol. **46**, 4 (2022).
6. A. Carena, V. Curri, P. Poggiolini, *et al.*, "Maximum reach versus transmission capacity for terabit superchannels based on 27.75-GBaud PM-QPSK, PM-8QAM, or PM-16QAM," IEEE Photonics Technol. Lett. **22**, 829 (2010).
7. M. Conti, S. Andrenacci, and N. Maturo, "Doppler impact analysis for NB-IoT and satellite systems integration," in *2020 IEEE International Conference on Communications (ICC)* (2020), p. 1.
8. Z. Zhao, M. Chen, X. Liu, *et al.*, "Compensation algorithm for reducing the influence of random vibration on fiber coupling in satellite laser communication," Opt. Commun. Technol. **44**, 47 (2020).
9. Y. Zhao and C. Jie, "Research on stray light suppression technology of optical system of laser communication terminal," Laser Infrared **51**, 1378 (2021).
10. A. E. Willner, K. Salman, C. M. Reza, *et al.*, "All-optical signal processing," J. Lightwave Technol. **32**, 660 (2013).
11. S. Marco, C. Sanghoon, P. Nicolay, *et al.*, "All-optical signal processing using dynamic Brillouin gratings," Sci. Rep. **3**, 1594 (2013).
12. M. Antonio, S. Mirco, M. Gianluca, *et al.*, "PPLN waveguide-based optical signal processing for next-generation networks," in *IEEE Photonics Society Summer Topical Meeting Series* (2014), p. 81.
13. C. Koos, P. Vorreau, T. Vallaitis, *et al.*, "All-optical high-speed signal processing with silicon–organic hybrid slot waveguides," Nat. Photonics **3**, 216 (2009).
14. L. Shao, F. Wen, B. Guo, *et al.*, "All-optical amplitude noise suppression in a nonlinear semiconductor optical amplifier (SOA)," in *Asia Communications and Photonics Conference* (2020), p. 298.
15. S. Surinder, S. Sukhbir, B. Nada, *et al.*, "Design and analysis of all-optical up- and down-wavelength converter based on FWM of SOA-MZI for 60 Gbps RZ data signal," Photonic Netw. Commun. **34**, 288 (2017).
16. T. T. Ng, A. Perez, S. Sales, *et al.*, "Characterization of XGM and XPM in a SOA-MZI using a linear frequency resolved gating technique," in *LEOS 2007-IEEE Lasers and Electro-Optics Society Annual Meeting Conference Proceedings* (2007), p. 656.
17. R. Baumgartner and R. Byer, "Optical parametric amplification," IEEE J. Quantum. Electron. **15**, 432 (1979).
18. D. M. Lai, C. Kwok, and K. K. Wong, "All-optical signal regeneration using optical parametric amplifier," in *Conference on Lasers and Electro-Optics and 2008 Conference on Quantum Electronics and Laser Science* (2008), p. 1.
19. R. Johann, K. Nikolai, J. Liu, *et al.*, "A photonic integrated continuous-travelling-wave parametric amplifier," Nature **612**, 56 (2022).
20. P. M. Gong, J. T. Hsieh, S. Lee, *et al.*, "Theoretical analysis of wavelength conversion based on four-wave mixing in light-holding SOAs," IEEE J. Quantum. Electron. **40**, 31 (2004).